



## Preclinical development of a high affinity anti-exatecan monoclonal antibody and application in bioanalysis of antibody-exatecan conjugates

Junshuang Xu<sup>a,1</sup>, Jing Wen<sup>a,1</sup>, Xiaobo Ji<sup>b</sup>, Jieru Chen<sup>b</sup>, Meiyu Yang<sup>b</sup>, Min Hong<sup>b,\*</sup>, Dawei Deng<sup>a</sup>

<sup>a</sup> China Pharmaceutical University, No. 639, Longmian Avenue, Jiangning District, Nanjing, Jiangsu Province 211198, China

<sup>b</sup> Shanghai Junshii Biosciences Co., Ltd. (TopAlliance), East of Gate 7, Yunchuang Road, Wujiang District, Suzhou, Jiangsu Province, China

### ARTICLE INFO

#### Keywords:

Exatecan  
Anti-exatecan antibody  
Bioanalysis  
Pharmacokinetics

### ABSTRACT

Exatecan, a topoisomerase I inhibitor, is currently utilized as a potent payload in antibody-drug conjugates, significantly enhances the efficacy and safety of these therapeutic agents. In the research of antibody-drug conjugates with exatecan as the payload conjugation, an anti-exatecan antibody serves as a crucial reagent for bioanalysis. In this study, BALB/c mice were immunized with bovine serum albumin conjugate exatecan (BSA-exatecan), and hybridoma technology was employed to screen seven hybridoma cell lines that stably express monoclonal antibodies. After evaluating their binding activity to exatecan, the cell line NO. 8B5-3H6 has been selected based on the EC<sub>50</sub> value. The antibody was purified using protein A affinity chromatography, resulting in a mouse anti-exatecan monoclonal antibody with a purity exceeding 99%. The binding profile with the exatecan demonstrated strong affinity, with an EC<sub>50</sub> of 1.382. Bio-Layer Interferometry (BLI) analysis further confirmed the high affinity of this mouse anti-exatecan antibody with a K<sub>D</sub> of less than 1 pM. Subsequently a detection method was developed using the mouse anti-exatecan antibody as the coating reagent and mouse anti-human IgG Fab conjugate HRP as the detection reagent. The standard curve and quantification range of the method were established at 31.25 ng/mL to 4000 ng/mL. Validation of accuracy, precision, selectivity, stability, dilution linearity, hook effect, parallelism and specificity were performed in accordance with ICH M10 and FDA bio-analytical method validation guidelines, laying a solid foundation for subsequent toxicological and pharmacokinetic studies of antibody-drug conjugate.

### 1. Introduction

The antibody-drug conjugate (ADC) class has emerged as one of the most rapidly expanding categories of tumor therapy in recent years, largely due to its favorable toxicity profile, extensive range of therapeutic applications, and high therapeutic window [1,2]. Up to now, 15 ADC drugs have received market approval, with many more currently in various stages of clinical trials [3]. Once ADC drugs enter the bloodstream and bind to the target antigen receptor on the surface of tumor cells, releasing the payload, that induces tumor cell death. The efficacy of ADC drugs is contingent upon the potency, toxicity, immunogenicity, stability, and functional groups of the payload [4]. Consequently, the ideal ADC payload has been the subject of considerable attention in this field. DNA inhibitors, as a type of ADC payload, target the entire cell cycle by damaging DNA through double-strand breaks, alkylation,

chimerism, cross-linking, and other mechanisms thereby producing cytotoxicity, which is a highly effective therapeutic effect against solid tumors [5]. Furthermore, it can also target tumor cells with low antigen expression [4]. A notable success in recent years has been the development of topoisomerase I (TOPO-I) inhibitors, with two topoisomerase I inhibitor-based ADCs approved by the FDA since 2019. The payload of trastuzumab deruxtecan (Enhertu®, DS-8201a) is an exatecan derivative (DXd), while that of sacituzumab govitecan (Trodelvy®) is the active metabolite SN28 of irinotecan [6,7]. In 2019, trastuzumab deruxtecan received FDA approval for the treatment of unresectable or metastatic HER2<sup>+</sup> breast cancer [8]. In 2021, it was approved for the treatment of advanced or metastatic HER2<sup>+</sup> gastric or gastroesophageal cancer [9]. In 2022, it was further approved for the treatment of unresectable or metastatic breast cancer [10]. Additionally, HER2<sup>+</sup> non-small cell lung cancer (Destination-Long02) has been included in the treatment

\* Corresponding author.

E-mail address: [hongminok@sjtu.edu.cn](mailto:hongminok@sjtu.edu.cn) (M. Hong).

<sup>1</sup> These authors contributed equally to the study.

<https://doi.org/10.1016/j.jpba.2025.116843>

Received 14 October 2024; Received in revised form 11 March 2025; Accepted 24 March 2025

Available online 2 April 2025

0731-7085/© 2025 Elsevier B.V. All rights reserved, including those for text and data mining, AI training, and similar technologies.

protocol. Furthermore, in April 2024, the FDA granted accelerated approval to Enhertu for the treatment of patients with unresectable or metastatic HER2<sup>+</sup> solid tumors [11]. This approval extends the availability of the drug across the entire spectrum of cancers, provided that patients with HER2<sup>+</sup> solid tumors are eligible for treatment.

Topoisomerase I is a pivotal nuclear enzyme that plays a crucial role in maintaining genome stability and preserving DNA structure. TOPO-I inhibitors have been linked to both innate and adaptive immune responses, indicating that ADCs targeting TOPO-I could offer potential benefits for antitumor immunotherapy [12]. The topoisomerase I inhibitor class of payloads includes both camptothecin-based and non-camptothecin-based compounds. The natural pentacyclic product camptothecin (CPT) induces apoptosis by binding to topoisomerase I and DNA, forming a robust complex that causes double-stranded DNA breaks in cells during the S phase of the cell cycle [4]. Exatecan mesylate (DX-8 951 f) is a water-soluble nonprodrug derivative of CPT that exhibits greater TOPO-I inhibition and antitumor activity than other CPT analogues [13]. Daiichi Sankyo achieved significant success with the development of a novel topoisomerase I inhibitor, a camptothecin derivative (DXd), by creating an ADC that conjugates DXd to an antibody via a tetrapeptide linker. The company has also established an extensive patent portfolio covering the ADC, DXd, and the associated linker-payload technology. In a fast-follow strategy, Hengrui Medicine developed several ADC drugs based on the DXd series, with the key difference being the introduction of a cyclopropyl group at the  $\alpha$ -position of the exatecan analogue amide [14]. Meanwhile, Chia Tai Tianqing has developed deuterated DXd-ADC (DDDxD) technology, effectively bypassing Daiichi Sankyo's patent protection on DXd. In studies with NCI-N87 tumor cells, deuterated DXd has shown stronger inhibitory activity against tumor cells compared to standard DXd [15]. Exatecan, a precursor to DXd, exhibits stronger cytotoxic effects, better permeability and a bystander killing effects compared to DXd. However, the extreme hydrophobicity of exatecan hinders its direct conjugation to antibodies, restricting its potential applications. In recent years, the development of exatecan derivatives and their applications in conjugation have led to a surge in patent filings. Baili pharms has applied for patents on exatecan derivatives that feature an R-configuration chiral carbon atom, which enhances water solubility [16]. Exatecan has been evaluated early in several clinical trials, however, the drug did not achieve favorable clinical outcomes due to a poor therapeutic window and dose-limiting toxicities including neutropenia, thrombocytopenia, and severe gastrointestinal side effects [17]. In the initial trials, exatecan was utilized as a warhead in conjunction with antibodies. However, considerable antibody aggregation was observed. Additionally, an *in vitro* study found that exatecan does not require a cyclohexyl amino ring (F-ring) to exert its antitumor effects, broadening the potential for functional group modifications to produce more linkable derivatives [18].

The bioanalysis of ADCs is a complex process influenced by several critical factors, including antibody affinity and specificity, the chemical properties of the payload, drug-to-antibody ratio (DAR) value, immunogenicity, and the generation of anti-drug antibodies (ADA), the primary method used the ligand-binding assay (LBA) to measure total antibody and ADC levels, while LC-MS/MS is typically employed for analyzing small molecule drugs. For the macromolecular portion of ADCs, ELISA indirectly estimates analyte concentrations based on the affinity between the analyte and the assay reagents [19]. During the early stages of ADC development, LBAs are favored for their high throughput and cost-effectiveness. However, these assays are often species-dependent [20], and their development necessitates the use of specialized reagents, including the preparation of monoclonal antibodies. Hybridoma technology serves as a crucial and potent approach for producing superior quality monoclonal antibodies. The foundational technology's initial establishment for monoclonal antibody production originated with Köhler and Milstein [21], who devised an effective approach for selecting newly fused hybridomas from a mixture of hybridomas, B cells, and non-fused tumor cells. Hybridoma technology

comprises several technical aspects, including antigen preparation, animal immunization, cell fusion, hybridoma screening and sub-cloning, and the identification and production of specific antibodies [22]. In actual cell fusion processes, PEG fusion agents, Sendai virus, or electrofusion are commonly used [23]. The electrofusion method utilizes short, strong pulses of an electric field to increase membrane permeability, inducing local perforations in the cell membrane that facilitate cell fusion, forming hybridomas [24].

BSA as an endogenous serum protein, demonstrates remarkable physicochemical properties. Therefore, BSA can be utilized as a carrier for conjugating exatecan, in preparation for the experiments of this study. The aim of this study is to manufacture a high-affinity mouse anti-exatecan monoclonal antibody (mAb) employing hybridoma technology. This mAb was subsequently used to establish a bioanalytical method for quantifying antibody-exatecan conjugates in cynomolgus monkey serum. The method was validated across several parameters, including standard curve, quantification range, accuracy, precision, selectivity, stability, dilution linearity, hook effect, parallelism and specificity. This provides a robust foundation for the bioanalysis of toxicology and pharmacokinetic (PK) studies.

## 2. Materials and methods

### 2.1. Materials

#### 2.1.1. Cell line and culture

The SP2/0 myeloma cell line, sourced from Junshi Biosciences, was revived from liquid nitrogen storage and cultured in RPMI 1640 complete medium containing 10 % fetal bovine serum (FBS) and 1 % pen strep (PS). The cells were incubated at 37°C with 5 % CO<sub>2</sub>, where they were expanded and passaged until reaching a bright, full state, ensuring sufficient cell quantity for the subsequent fusion process.

#### 2.1.2. Animals and husbandry

Female BALB/c mice, aged 6–8 weeks (SPF grade) and weighing (20 ± 2) g, were purchased from Hangzhou Qingzhen Experimental Animal Technology Co., Ltd. The animals were housed in an SPF-grade facility at Immune Tech company (Suzhou, China) (No. SYXK (Su) 2021–0071). The housing conditions were maintained at a temperature of 20–26°C, relative humidity of 40 %–70 %, with a pressure differential of 10–40 Pa, a 12 h light/dark cycle, and at least 10 air changes per hour with fresh air. Food and water were provided *ad libitum*. All animal care and handling were conducted in accordance with Good Laboratory Practice (GLP) guidelines. This study adhered to all relevant local, national, and international animal welfare standards, with protocols approved by the Institutional Animal Care and Use Committee (IACUC). The IACUC number is 202401.

#### 2.1.3. Reagents and equipment

BSA-exatecan [25] and Anti-KLH IgG1-Exatecan-DAR8 (purity 97.5 %) were prepared by Junshi Biosciences, the biochemical structure of BSA-exatecan and anti-KLH IgG1-Exatecan DAR8 ADC was shown in Fig. 2A and Supplementary Figure A (BSA-exatecan is a conjugate of bovine serum albumin with an average of 4.7 CPD1 molecules, where CPD1 refers to a linker-payload described in a patent, include a hydrophilic linker and exatecan, synthesized by personnel at Junshi Biosciences, following an established laboratory protocol, Suzhou, China). Freund's complete adjuvant and Freund's incomplete adjuvant were purchased from Biodragon company (Suzhou, China). HAT medium, Pen strep, RPMI 1640 medium and HT medium were ordered from Gibco (Grand Island, NY, USA). Fetal bovine serum was obtained from Royacel company (Lanzhou, China). Cell electrofusion buffer was purchased from Qiwen biotech (Shanghai, China). Goat anti-mouse IgG(H+L) secondary antibody HRP was acquired from Invitrogen (Cat.No:31430, Carlsbad, CA, USA). TMB microwell peroxidase substrate (1-Component) were purchased from Seracare Life Sciences (Cat.No:5120–0077,

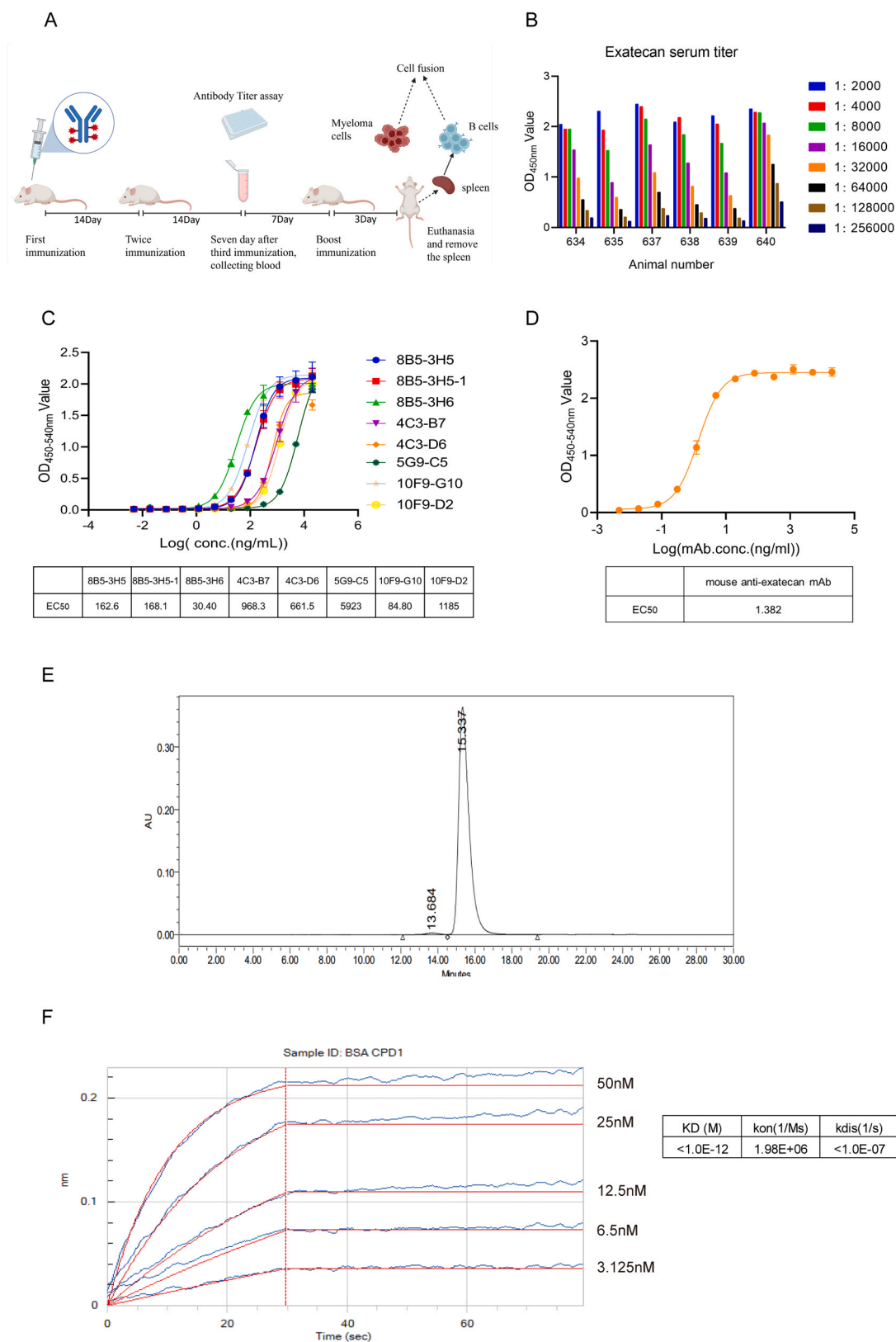


**Fig. 1.** Preparation of mouse anti-exatecan mAb. **A.** Mouse immunization flowchart. **B.** Antibody titer of mouse serum after three immunizations, starting with a 1:2000 dilution and subsequently doubling serial dilutions. **C.** Binding activity of antibodies produced by the seven positive hybridoma cell lines was evaluated with BSA-exatecan. **D.** The binding profile of the mouse anti-exatecan antibody was obtained from monoclonal cell lines through sequencing, plasmid construction, transient transfection, culturing, and final purification. **E.** Chromatogram of mouse anti-exatecan antibody detected by SEC-HPLC after purification. **F.** Binding process of gradient-diluted BSA-exatecan to 2 µg/mL mouse anti-exatecan antibody, due to the tight binding affinity between the two molecules, dissociation proved challenging, leading to an inability to successfully fit the  $K_{dis}$  curve.

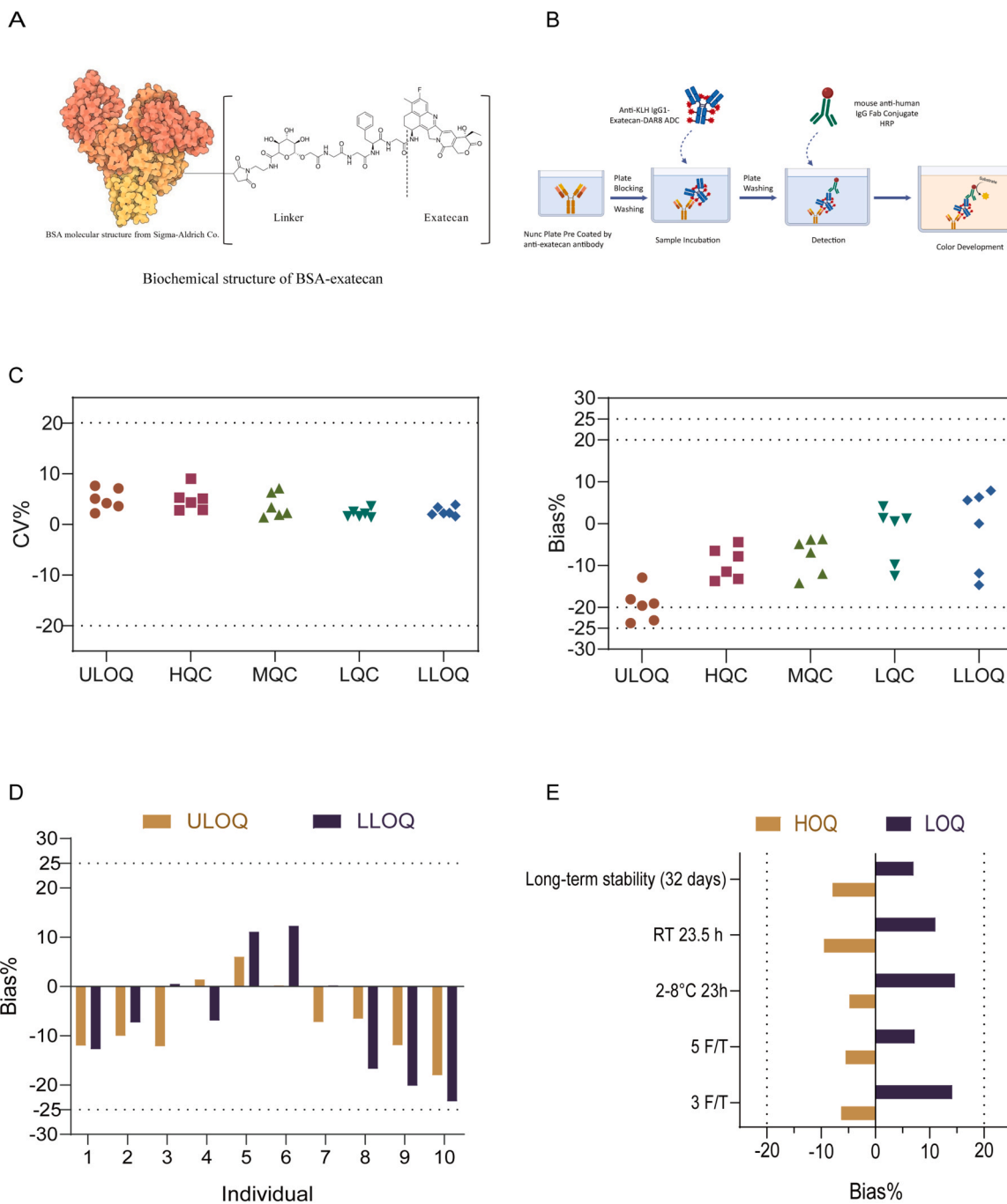


**Fig. 2.** Method development and validation for antibody-exatecan conjugates. A. The biochemical structure of BSA-exatecan. B. Bioanalysis development flowchart of antibody-exatecan conjugates. C. Intra-assay accuracy and precision, six runs of five QCs with different concentrations were analyzed with the assay, involving three sets of QCs for each run, and two replicates for each set, the dotted lines represent the acceptance limits of CV% and Bias%. D. Selectivity evaluation of ADC, ten lots of naive serum samples were used for selectivity evaluation, the dotted lines represent the acceptance limits of the ULOQ and LLOQ-level samples, respectively. E. Sample stability evaluation, the stability of HQC and LQC samples was tested under various storage conditions, with each sample tested three times, the dotted lines represent the acceptance limits of the HQC and LQC level samples, respectively.

Milford, MA, USA). Bovine serum albumin (BSA) was obtained from Sigma-Aldrich (Saint Louis, MO, USA). Mouse anti-human IgG Fab conjugate HRP mAb were purchased from GenScript company (Cat.No: A01855, Nanjing, China). Protein A affinity chromatography column was received from Cytiva company (Marlborough, MA, USA). Nunclon delta surface cell culture plastics, Nunc-Immuno 96 microplate and CO<sub>2</sub> incubator from Thermo Fisher Scientific (Waltham, MA, USA). Microplate reader SpectraMax M5 were ordered from Molecular Devices company (San Jose, CA, USA). Electro cell manipulator was purchased

from BTX company (Holliston, MA, USA). Octet RED96e were purchased from Sartorius Fortebio (Niedersachsen, Germany).

## 2.2. Methods

### 2.2.1. Preparation of monoclonal antibody

**2.2.1.1. Mouse immunization.** Six female BALB/c mice aged six to eight weeks, the BSA-exatecan was diluted in saline to a concentration of

2 mg/mL and mixed with Freund's adjuvant in a 1:1 ratio. Each mouse was subcutaneously immunized with a dose of 100  $\mu$ g. Booster immunizations were administered at 14-day intervals. Seven days after the third immunization, blood was collected to obtain serum samples. The immune response of the mice was evaluated using indirect ELISA, and those with high antibody titers were selected for subsequent experiments. Prior to fusion, the selected mice received a final intraperitoneal immunization boost. The protocol for the above immunization method as previously described [26].

**2.2.1.2. Cell fusion.** After evaluating the antibody titers of the immunized mice, the mouse with the highest antibody titer was selected for fusion. The selected mouse was euthanized, and its spleen was harvested under a laminar flow hood. The spleen was ground and filtered to obtain spleen cells. After lysing the red blood cells mixed with the spleen cells, the spleen cells were mixed with SP2/0 myeloma cells at a 4:1 ratio and then fused. Electrofusion technology (BTX Electro cell manipulator) was employed to fuse the mouse spleen cells with SP2/0 myeloma cells, forming hybridoma cells. The hybridoma cells were cultured in HAT selection medium in a humidified incubator at 37°C with 5 % CO<sub>2</sub> for 4–7 days to observe the fusion status, with media changes as necessary. Approximately 12 days later, the culture supernatant was collected and tested using an established ELISA method for all wells.

**2.2.1.3. Cloning and screening of hybridoma cells.** The cell supernatant was initially screened using ELISA method coated with BSA-exatecan to identify positive wells. Based on the detection results, 36 cell clones were selected for subcloning. To prevent hybridoma cells from losing the ability to secrete antibodies due to chromosomal loss as the number of replications increases, subcloning is necessary. After subcloning, stable monoclonal cell lines can be obtained. Subcloning: nourishing layer cells were pre-plated onto 96-well plates at 100  $\mu$ L per well. The 36 selected positive cells were then subjected to limiting dilution, and the cell suspension was added to the 96-well plates at 100  $\mu$ L per well, ensuring approximately 90 cells per subcloning plate, with no more than one cell per well. The cells were cultured in HT complete medium for 12–14 days. After this period, ELISA screening was performed to select positive monoclonal cell lines. Through repeated screening and testing, positive monoclonal cell lines 8B5–3H5, 8B5–3H6, 4C3–B7, 4C3–D6, 5G9–C5, 10F9–G10, and 10F9–D2 were identified for expansion and cultivation.

**2.2.1.4. Monoclonal antibody purification.** The 8B5–3H6 hybridoma cell line was subjected to mass cultivation and subsequently transferred to hybridoma serum-free medium for antibody expression. The cell supernatant was harvested seven days following the transfer for protein purification. Protein A was connected to the AKTA avant purifier, and the pipeline was initially self-checked. Subsequently, the pipeline was washed and flushed with 0.1 M sodium hydroxide to remove potential protein residues within the pipeline and column. Thereafter, the column was equilibrated with buffer PBS. Sampling was conducted through a 100 % A pump at a rate of 2 mL/min, and the pH 2.5 glycine elution was performed to collect the antibody. The purification method was developed based on the procedure described by C. Hollander et al. [27].

**2.2.1.5. Characterization of the anti-exatecan antibody.** The concentration of the sample was determined using a nanodrop spectrophotometer, and the purity was assessed using size-exclusion high-performance liquid chromatography (SEC-HPLC) and a 100  $\mu$ L sample of mouse anti-exatecan mAb was injected into a chromatography column (XBridge® BEH200A SEC, 3.5  $\mu$ m) and eluted at a constant flow rate. The proteins were separated based on their size and detected by the chromatography system's detector. After confirming the purity of the eluted fractions, a buffer exchange was performed to obtain the purified mouse anti-exatecan monoclonal antibody. For the binding of exatecan, purified mouse anti-exatecan mAb was serially diluted starting at fourfold.

Coating was done with 1  $\mu$ g/mL anti-KLH IgG1-Exatecan-DAR8 (ADC molecule of exatecan), and detection was performed with anti-mouse IgG(H+L) secondary antibody HRP diluted 1:5000 in 2 % BSA-PBS buffer. TMB substrate solution was used for color development, and the reaction was stopped by adding 1 M sulfuric acid. Data were read on a microplate reader at 450 nm with a reference wavelength of 540 nm. In the determination of the affinity constant between mouse anti-exatecan mAb and BSA-exatecan, the Octet Red 96 molecular interaction analyzer was used to measure the K<sub>D</sub> value. Protein A probes were equilibrated in PBST buffer at room temperature prior to the experiment. BSA-exatecan was serially diluted to five concentration levels: 50 nM, 25 nM, 12.5 nM, 6.25 nM, and 3.125 nM. The mouse anti-exatecan mAb sample was prepared at a concentration of 2  $\mu$ g/mL. Both the BSA-exatecan dilutions and the mAb samples, along with the PBST buffer, were added to the sample plate, with 200  $\mu$ L per well. The assay was conducted according to the instrument's programmed settings to measure the K<sub>D</sub> value.

## 2.2.2. Development and validation of bioanalysis method

**2.2.2.1. Development of anti-KLH IgG1-Exatecan-DAR8 ADC bioanalysis assay.** A 96-well plate was coated with 1  $\mu$ g/mL mouse anti-exatecan mAb and incubated overnight at 2–8°C for 16–20 h. After incubation, the coated plate was washed with PBS (pH 7.3) containing 0.05 % (v/v) Tween-20 washing solution, 300  $\mu$ L per well for four times. Each well was then blocked with 200  $\mu$ L of 3 % BSA-PBS blocking solution for 2 h. After washing, 100  $\mu$ L of diluted calibrators and QCs were added to each well. The calibrators and quality controls (QCs) were prepared from a 5.82 mg/mL stock solution of anti-KLH IgG1-Exatecan-DAR8 ADC, which was initially diluted with buffer to obtain a 120  $\mu$ g/mL solution. This solution was further diluted in monkey serum to achieve the target concentrations and subsequently diluted with assay buffer at a minimum required dilution (MRD) of 40 before being added to the ELISA plate. The plate was incubated at room temperature with shaking at 500 rpm for 1 h. Following another wash cycle (four times), the analytes in the samples bound to the mouse anti-exatecan mAb. Then, 100  $\mu$ L/well of mouse anti-human IgG Fab conjugate HRP (diluted 1:4000 in 1 % BSA-PBS) was added as the detection antibody and incubated at room temperature with shaking at 500 rpm for 1 h. After washing the plate, 100  $\mu$ L/well of TMB substrate solution was added for color development, and the plate was stored in the dark at room temperature for 5–10 min. The reaction was stopped by adding 50  $\mu$ L of 1 M sulfuric acid per well. OD values were read at 450 nm with a reference wavelength of 630 nm on microplate reader. The concentration of the analyte was plotted on the x-axis, and the difference in OD values between the duplicate analyte wells and the duplicate blank wells was plotted on the y-axis. A four-parameter logistic equation was used to fit the standard curve, and sample concentrations were calculated using SoftMax Pro 7.3 software.

**2.2.2.2. Validation of anti-KLH IgG1-Exatecan-DAR8 ADC bioanalysis method.** Validation experiments of bioanalysis method include parameters such as standard curve and quantification range, accuracy and precision, selectivity, stability, dilution linearity and hook effect, parallelism and specificity. The acceptance criteria for bias (Bias%), coefficient of variation (CV%), and total error (TE%) in the following described parameters of accuracy and precision, selectivity, stability, dilution linearity and hook effect, parallelism and specificity comply with the US FDA and ICH M10 bioanalytical method validation guidelines [28,29]

**2.2.2.2.1. Standard curve and quantification range.** In this validation, calibration standards and quality controls were prepared using pooled blank serum from at least 10 individual cynomolgus monkeys. The quantitation range for detecting anti-KLH IgG1-Exatecan-DAR8 ADC was 31.25 ng/mL to 4000 ng/mL. The concentrations of calibration

curve samples were as follows: 4000 ng/mL (ULOQ), 2000 ng/mL, 1000 ng/mL, 500 ng/mL, 250 ng/mL, 125 ng/mL, 62.5 ng/mL, 31.25 ng/mL (LLOQ), 15.625 ng/mL (anchor point L) and 0 ng/mL (pooled cynomolgus monkeys blank serum sample without anti-KLH IgG1-Exatecan-DAR8 ADC). The concentrations of QC samples were HQC (3000 ng/mL), MQC (450 ng/mL), LQC (90 ng/mL). To plot the standard curve of anti-KLH IgG1-Exatecan-DAR8 ADC using OD values and concentrations, fitting the four-parameter logistic regression model:  $Y = (A-D)/[1 + (x/C)^B] + D$ , A: Estimation of asymptote under curve, D: Estimation of asymptote above curve, B: Slope of curve, C: Concentration of half combination.

**2.2.2.2. Accuracy and precision.** The accuracy and precision assessments were carried out at concentrations of 4000 ng/mL, 31.25 ng/mL, 3000 ng/mL, 450 ng/mL, and 90 ng/mL, representing ULOQ, LLOQ, HQC, MQC, and LQC, respectively. These tests were performed by at least two analysts over at least two days, with a minimum of six independent assays, each involving triplicate measurements of the samples. If the bias for HQC, MQC, and LQC samples is within  $\pm 20\%$  of the standard concentration, deviations of  $\pm 25\%$  are suitable for ULOQ and LLOQ. The coefficient of variation for accuracy and precision should be  $\leq 20.0\%$  for HQC, MQC, and LQC samples, and  $\leq 25.0\%$  for ULOQ and LLOQ. The total error should be within limits of  $30.0\%$  (not exceeding  $40.0\%$  for ULOQ and LLOQ), meeting the acceptance criteria. To ensure intra-assay accuracy and precision, at least 2 out of 3 runs must adhere to the established criteria.

**2.2.2.3. Specificity.** Specificity validation experiments involved preparing spiked cynomolgus monkey serum with increasing concentrations of naked antibody sample (anti-KLH-IgG1) at 200  $\mu\text{g/mL}$  and 25  $\mu\text{g/mL}$ , as well as a small molecule sample (exatecan) at 10 ng/mL, along with standard samples for ADC-specific detection. HQC and LQC were tested in duplicate at these concentrations five times. Acceptance criteria were met if at least 80% of the samples for HQC and LQC had Bias% within  $\pm 20.0\%$ , and the OD values for blank matrix measurements were below the quantification limit OD value.

**2.2.2.4. Selectivity.** The selectivity validation assay involved preparing ULOQ and LLOQ samples using individual serum from at least 10 cynomolgus monkeys. Acceptance criteria were met if the OD values of blank matrix measurements without standard additions were below the OD value of LLOQ, and if at least 80% of samples for ULOQ and LLOQ had Bias% within  $\pm 25.0\%$ .

**2.2.2.5. Stability.** The stability assessment involved using HQC and LQC standards prepared from pooled serum of cynomolgus monkeys to evaluate stability after 3 and 5 freeze-thaw cycles, short-term stability at  $2-8^\circ\text{C}$  in a medical refrigerator and at room temperature for 24 h, and long-term stability at  $-70$  to  $-90^\circ\text{C}$  for one month. Each stability test included triplicates of HQC and LQC samples. Acceptance criteria were met if the Bias% for HQC and LQC in stability testing was within  $\pm 20.0\%$ .

**2.2.2.6. Dilution linearity and hook effect.** In the assay of dilution linearity, anti-KLH IgG1-Exatecan-DAR8 ADC at 5.82 mg/mL was diluted with pooled blank serum of cynomolgus monkeys to obtain final concentrations of 2318 ng/mL, 582 ng/mL, and 145.5 ng/mL at dilution factors of 1:2500, 1:10000, and 1:40000, respectively, each prepared in five sets. Acceptance criteria were met if the Bias% between the mean measured concentrations and theoretical concentrations at each dilution factor fell within  $\pm 20.0\%$ , and if the CV% of the recalculated final concentrations from all dilution samples at the same concentration did not exceed  $20.0\%$ . For the hook effect assessment, starting from the concentration of 5.82 mg/mL, samples were diluted 20-fold and 200-fold to achieve concentrations of 291  $\mu\text{g/mL}$  and 29.1  $\mu\text{g/mL}$ , respectively. The absence of a hook effect was confirmed if the OD values of verification samples at concentrations above the ULOQ were not lower than the ULOQ OD value.

**2.2.2.7. Parallelism.** Parallelism evaluates the consistency between the calibration curve and serially diluted biological samples, assessing the impact of dilution on analyte measurement. High-dose

biological samples, preferably near Cmax, should be serially diluted to at least three concentrations, with each dilution performed in triplicate. The CV% within each dilution series should not exceed  $30\%$ . The parallelism experiment was conducted using serum samples obtained from cynomolgus monkey in a toxicity study of an ADC targeting EGFR and HER3, with exatecan as the payload. The serum sample was collected from a male animal in the high-dose group (30 mg/kg) at the Cmax time point (immediately post-dose  $\pm 1$  min). This toxicity study was performed at Shanghai Innostar Biotech Co., Ltd. However, since the study data have been utilized for IND application purposes and are subject to confidentiality requirements, further details cannot be disclosed. The parallelism experiment was conducted using the quantitative ADC assay developed, with mouse anti-exatecan mAb as the coating reagent. The detailed methodology is provided in the supplementary materials.

### 2.3. Data analysis

The data presented in this study were gathered and subjected to analysis using the SoftMax Pro 7.3 software, which is provided with the microplate reader. A four-parameter logistic model was employed for data analysis and curve fitting. GraphPad Prism 8 software was utilized for statistical evaluation. The figure was completed by BioRender.

## 3. Results and discussion

### 3.1. Mouse antibody titer assay

BALB/c mice (SPF grade) represent the predominant animal strain utilized for the generation of monoclonal antibodies, primarily because most murine myeloma cells used for cell fusion, including SP2/0, originate from this strain. Therefore, six BALB/c mice were immunized with the BSA-exatecan (immunization flowchart show in Fig. 1A). On the seventh day after the third immunization, blood was collected from the eye sockets of the mice to obtain serum, and the antibody titers in the serum were detected using an established ELISA method (as shown in Fig. 1B). The results indicated that the sera from all six mice were able to bind to the coated BSA-exatecan. Based on the experimental results, mouse 640 showed an antibody titer of 1:256000, which was superior to the other animals. Therefore, mouse 640 was selected for subsequent fusion and screening experiments.

### 3.2. Manufacturing, subcloning and screening of hybridoma cells

The cells from mouse number 640 were fused, and the cell supernatant was tested using the ELISA method to screen for positive cells after fusion. Positive cells were selected and subjected to limited dilution for subcloning. Supplementary Figure B shows the ELISA detection results of the cell supernatants after subcloning, indicating that more than 40 positive monoclonal cells were identified. These positive monoclonal cells were then expanded in culture. Through a process of subcloning, detection, screening, and retesting, seven positive hybridoma cell lines that could stably express antibodies were ultimately selected: 8B5-3H5, 8B5-3H6, 4C3-B7, 4C3-D6, 5G9-C5, 10F9-G10, and 10F9-D2. These cell lines were then tested using ELISA plates coated with BSA-exatecan. The results indicated that all the selected cell lines bound to BSA-exatecan (as shown in Fig. 1C). Among them, the 8B5-3H6 cell line had the lowest  $\text{EC}_{50}$  values of 30.40. Therefore, the antibody expressed by this cell line was selected for further antibody production.

### 3.3. Preparation and functional characterization of anti-exatecan monoclonal antibody

The supernatant from cultured monoclonal cell lines, after sequencing, plasmid construction, and transient transfection, was collected and purified using protein chromatography to obtain mouse

anti-exatecan mAb. The purity of the purified monoclonal antibody was assessed using SEC-HPLC. As shown in Fig. 1E, the monomer peak appeared at 15.337 min with a peak area of 99 %, while a minor aggregate peak was observed at 13.684 min, accounting for less than 1 % of the total peak area. These results indicate that the purity of the mouse anti-exatecan antibody is 99 %. The purified mouse anti-exatecan mAb was characterized to confirm its biological function, and ELISA was used to verify its binding activity to exatecan. As shown in Fig. 1D, the results demonstrate that the anti-exatecan mAb has a good binding profile with anti-KLH IgG1-Exatecan-DAR8, with an  $EC_{50}$  of 1.382. As illustrated in Fig. 1F, the binding profile of BSA-exatecan with the mouse anti-exatecan mAb, measured using the Octet Red molecular interaction analyzer, shows that increasing concentrations of BSA-exatecan result in enhanced binding to the antibody. By analyzing the binding and dissociation curves across different BSA-exatecan concentrations, the  $K_D$  value was determined to be less than  $1.0E^{-12}$ , with a fitted curve showing a correlation coefficients ( $R^2$ ) value of 0.993. This indicates that the mouse anti-exatecan mAb exhibits a high affinity for BSA-exatecan.

### 3.4. Methodological validation

We utilized the prepared mouse anti-exatecan mAb to develop a method for detecting anti-KLH IgG1-Exatecan-DAR8 ADC concentration in monkey serum (flowchart show in Fig. 2B) and validated this method. The validation adhered to the guidelines for the quantitative analysis of biological samples as outlined in the FDA Bioanalytical Method Validation 2018 and M10 Bioanalytical Method Validation and Study Sample Analysis 2022 (ICH M10) bioanalytical method validation guidelines.

#### 3.4.1. Standard curve

For the standard curve of the method to detect anti-KLH IgG1-Exatecan-DAR8 ADC concentration in monkey serum, we used a four-parameter logistic model for fitting (show Supplementary Figure C), A representative standard curve is presented in, with  $R^2$  ranging from 0.996 to 1.000, indicating a good fit. From the six validation batches of this detection method, the Bias% range for ULOQ and LLOQ samples was  $-10.7$ – $11.6$  %, with CV% values not exceeding 15.9 %. For other standards, the Bias% range was  $-6.4$ – $11.6$  %, with CV% values ranging from 0 % to 8.1 %, demonstrating the standard curve's good reproducibility.

#### 3.4.2. Accuracy and precision

Fig. 2C presents the results of the method validation for accuracy and precision, which were evaluated by at least two individuals over six independent analysis batches. Each sample concentration of ULOQ, LLOQ, HQC, MQC, and LQC was tested in quintuplicate, and the results were averaged. Table 1 shows the inter-batch accuracy and precision results, with Bias% and CV% ranges of  $-9.5$  % to  $-2.5$  % and  $2.1$ – $4.9$  %, respectively (ULOQ and LLOQ results were  $-19.4$  % to  $-1.1$  % and  $2.6$ – $5.0$  %). Within each analysis batch, the Bias% ranged from  $-14.2$ – $4.1$  %, and CV% values ranged from 1.4 % to 9.0 % (ULOQ and LLOQ Bias% and CV% were  $-23.8$ – $7.9$  % and  $1.6$ – $7.6$  %, respectively). For TE% of the method, the intra-batch range was  $2.6$ – $20.6$  % (ULOQ

**Table 1**  
Inter-assay accuracy and precision.

Analyte	Sample	Nominal Conc. (ng/mL)	CV%	Bias%	TE%
Inter-run	ULOQ	4000.000	5.0	$-19.4$	24.4
	HQC	3000.000	4.9	$-9.5$	14.4
	MQC	450.000	3.8	$-7.6$	11.4
	LQC	90.000	2.1	$-2.5$	4.6
	LLOQ	31.250	2.6	$-1.1$	3.7

Note: six independent runs involved three sets of QCs for each run and two replicates for each set. Conc = concentration, CV%: Coefficient of variation, deviation between each measurement, TE%: Total system error, TE% = ( $|Bias|$  % + CV%).

and LLOQ values were  $2.2$ – $31.0$  %), and the inter-batch range was  $4.6$ – $14.4$  % (ULOQ and LLOQ values were  $3.7$ – $24.4$  %), indicating that the results fulfilled the acceptance criteria.

#### 3.4.3. Specificity

The specificity assessment results for anti-KLH IgG1-Exatecan-DAR8 ADC are shown in Table 2 and Table 3. These tables illustrate the interference effects of the naked antibody anti-KLH-IgG1 and the small molecule exatecan on the ADC. The Bias% values for the HQC and LQC samples satisfied the accepted standards, with anti-KLH-IgG1 values ranging from  $-7.2$ – $0.3$  % and  $0.9$ – $12.4$  %, respectively. When exatecan was added, over 80 % of the Bias% values met the criteria, ranging from  $-17.1$  % to  $-1.5$  % and  $12.7$ – $16.3$  %. The blank matrix samples without the addition of anti-KLH IgG1-Exatecan-DAR8 ADC standard showed values below the lower limit of quantification. These results indicate that the coating antigen and the detection antibody can specifically recognize the standard without interference from structurally similar substances, anti-KLH-IgG1 at concentrations up to  $200$   $\mu$ g/mL and exatecan at concentrations up to  $10$  ng/mL, ensuring accurate detection of the target analyte in the serum.

#### 3.4.4. Selectivity

Fig. 2D shows the detection results of ULOQ and LLOQ samples prepared in individual serum from 10 cynomolgus monkeys. The Bias% range for ULOQ was  $-18$ – $6.0$  %, and for LLOQ, it was  $-23.3$ – $12.3$  %. The signal values for the blank matrix without added standards were all below the lower limit of quantification. This indicates that the method ensures precise quantification of the analyte in serum matrices even in the presence of non-structurally related substances, with no non-specific interference.

#### 3.4.5. Dilution linearity and hook effect

Table 4 shows the results of the dilution linearity test. The initial concentration of the standard,  $5.82$  mg/mL, was diluted to the respective ratios (i.e., 2500-fold, 10000-fold, and 40000-fold) using mixed cynomolgus monkey blank serum. Five sets were prepared for each dilution ratio. The Bias% values for each dilution ranged from  $-15.6$ – $9.7$  %, with CV% not exceeding 3.7 %. This indicates that the samples can be accurately detected within the maximum dilution range of 40000-fold.

Table 5 presents the results of the hook effect experiment. Samples diluted 20-fold and 200-fold resulted in final concentrations of  $291$   $\mu$ g/mL and  $29.1$   $\mu$ g/mL, respectively, with each concentration tested in five replicates. The results demonstrate that the signal values of these concentrations, which exceed the ULOQ ( $291$   $\mu$ g/mL range), show no significant decrease compared to the signal values at the ULOQ

**Table 2**

Specificity of anti-KLH IgG1-Exatecan-DAR8 ADC determination in serum samples with anti-KLH-IgG1.

Anti-KLH-IgG1 ( $\mu$ g/mL)	BL	HQC		LQC	
		3000.000(ng/ mL)	Bias %	90.000(ng/ mL)	Bias %
200.000	BQL	2845.744	$-5.1$	100.299	11.4
	BQL	2882.538	$-3.9$	101.177	12.4
	BQL	2964.422	$-1.2$	96.898	7.7
	BQL	3008.284	0.3	98.009	8.9
	BQL	2925.077	$-2.5$	93.465	3.9
25.000	BQL	2800.578	$-6.6$	95.994	6.7
	BQL	2783.897	$-7.2$	95.763	6.4
	BQL	2828.229	$-5.7$	95.995	6.7
	BQL	2942.137	$-1.9$	97.477	8.3
	BQL	2996.529	$-0.1$	90.769	0.9

Note: ADC samples prepared from pooled cynomolgus monkey serum previously spiked with anti-KLH-IgG1 of  $200$   $\mu$ g/mL or  $25$   $\mu$ g/mL, each concentration was tested across five separate experiments. BQL: Below the quantity limits.

**Table 3**

Specificity of anti-KLH IgG1-Exatecan-DAR8 ADC determination in serum samples with exatecan.

Exatecan (ng/mL)	BL 0.000(ng/mL)	HQC		LQC	
		3000.000(ng/mL)	Bias%	90.000(ng/mL)	Bias%
10.000	BQL	2730.130	-9.0	104.696	16.3
	BQL	2630.940	-12.3	101.444	12.7
	BQL	2488.277	-17.1	108.051	20.1*
	BQL	2587.018	-13.8	103.806	15.3
	BQL	2954.156	-1.5	101.701	13.0

Note: ADC samples prepared from pooled cynomolgus monkey serum previously spiked with exatecan of 10 ng/mL, each concentration was tested across five runs. BQL: Below the quantity limits. \*: Bias% not meet the acceptance criteria.

concentration. No hook effect was observed.

### 3.4.6. Stability

In different stability conditions, HQC and LQC samples underwent stability testing three times each, as shown in Fig. 2E. The Bias% of the tested samples under conditions of three freeze-thaw cycles, five freeze-thaw cycles, room temperature exposure for 23.5 h, refrigerator storage at 2–8°C for 23 h, and ultra-low temperature freezer storage (-70 to -90°C) for 30 days all met the acceptance criteria. These results indicate that HQC and LQC samples are stable under the specified storage conditions.

### 3.4.7. Parallelism

Table 6 presents the results of the parallelism assessment. A high-dose biological sample, near C<sub>max</sub>, was diluted 500-fold, 1000-fold, and 2000-fold for analysis. The results showed that the sample concentrations remained within the quantification range, with a CV% of

7.8 %. This demonstrates that the analyte can be accurately quantified even after serial dilutions, confirming the parallelism of the bio-analytical method.

In this investigation, the authors present the generation, selection, and screening processes of anti-exatecan antibody by using hybridoma technology, as well as the successful development of high-affinity mouse anti-exatecan mAb. Furthermore, a bioanalytical method for the anti-KLH IgG1-Exatecan-DAR8 ADC was developed and validated in accordance with the analytical method validation guidelines set forth by the ICH M10 and FDA bioanalytical method validation. By subcutaneously immunizing BALB/c mice with BSA-exatecan and conducting multiple immunizations, induced the production of antibodies. One week after the third immunization, assessed the antibody titers in mice. ELISA results demonstrated that all mouse serum antibodies exhibited good binding to BSA-exatecan, confirming the success of the immunization protocol. Among the six mice, mouse numbered 640 exhibited the highest antibody titer. Consequently, we selected this mouse for subsequent cell fusion experiments. We fused splenocytes from mouse 640 with SP2/0 myeloma cells using electrofusion technology to produce hybridoma cells. After culturing, we selected and screened positive cells through ELISA, resulting in the subcloning of positive cells. Ultimately, we selected seven positive cell lines: 8B5-3H5, 8B5-3H6, 4C3-B7, 4C3-D6, 5G9-C5, 10F9-G10, and 10F9-D2. These seven positive cell lines were continuously expanded to secrete anti-exatecan monoclonal antibodies. Serial dilution assays of the secreted antibodies showed that 8B5-3H6 had the lowest EC<sub>50</sub> values of 30.40. This clone was sequenced, and the plasmid was constructed, followed by transient transfection and culturing of cells. The supernatant was purified using a protein A affinity column, yielding a final concentration of 0.7 mg/mL of mouse anti-exatecan monoclonal antibody. By characterizing the antibody, it was determined that the antibody has a purity of 99 %. It exhibited a good binding profile with anti-KLH IgG1-Exatecan-DAR8,

**Table 4**

Dilutional linearity of anti-KLH IgG1-Exatecan-DAR8 ADC in drug-free serum samples assessed by precision and accuracy.

Initial Conc. (mg/mL)	Dilution Factor	Nominal Conc. (ng/mL)	Back-calculate Concentration (ng/mL)					Mean	Bias%	CV%
			Run 1	Run 2	Run 3	Run4	Run5			
5.820		2328.000	1798.979	1932.127	1915.681	2085.138	2090.464	1964.478	-15.6	3.7
	2500									
	10000	582.000	580.127	551.494	518.811	519.809	580.284	550.105	-5.5	
	40000	145.500	156.520	158.992	167.624	159.976	155.035	159.629	9.7	

Note: three samples (five sets per sample) at concentrations (145.5, 582 and 2328 ng/mL) diluted respectively with assigned dilution factors (2500, 10000 and 40000-fold) were analyzed to assess the dilutional linearity. Conc = concentration.

**Table 5**

Hook effect of anti-KLH IgG1-Exatecan-DAR8 ADC determination of extremely high concentrations in serum samples.

Dilution Factor	Nominal Conc. (ng/mL)	OD value					Mean
		Run 1	Run 2	Run 3	Run4	Run5	
20	291000.000	3.069	3.092	3.091	3.198	3.127	3.115
200	291000.000	3.116	3.072	3.035	3.106	3.040	3.074
ULOQ	4000.000	NA	NA	NA	NA	NA	3.095

Note: two samples (five sets per sample) at high nominal concentrations (29.1 and 291 µg/mL) diluted with serum were analyzed to assess the hook effect. Conc = concentration, NA: Not Applicable.

**Table 6**

Parallelism validation of assay.

Analyte	Dilution Factor	Measured Conc. (ng/mL)			Mean Conc. (ng/mL)	CV%
		Run 1	Run 2	Run 3		
T411-11	500	665997.842	665250.063	662803.662	664683.856	7.8
	1000	747261.686	736669.217	771219.126	751716.676	
	2000	735429.919	794672.431	786266.410	772122.920	

Note: T411-11 is the identification number for the biological sample. Conc = concentration, CV%: Coefficient of variation, deviation between each measurement.

with an  $EC_{50}$  of 1.382, and demonstrated a strong affinity to BSA-exatecan, with a  $K_D$  value of less than  $1.0E^{-12}$ .

The guidance “Clinical Pharmacology Considerations for Antibody-Drug Conjugates Guidance for Industry” issued by the FDA in 2024 emphasizes that multiple analytes should be measured during the bioanalysis of ADC drugs to evaluate ADC exposure. These include the total antibody content, the ADC content, and the concentrations of the small molecule payload and pharmacologically active metabolites [30,31]. In this study, we developed an ELISA method for the quantitative analysis of ADC samples using an anti-payload antibody reagent. The anti-exatecan antibody produced by hybridomas was used as a coating reagent to capture samples from cynomolgus monkey serum. This assay is sensitive and specific, with a quantitation range of 31.25 ng/mL to 4000 ng/mL. During the analytical method development process, we conducted a systematic exploration and optimization phase. The coating concentration of anti-exatecan mAb was evaluated at 0.5  $\mu$ g/mL, 1  $\mu$ g/mL, and 2  $\mu$ g/mL, and considering the standard’s characteristics and source, mouse anti-human IgG Fab Conjugate HRP was chosen as the detection antibody. Its concentration was optimized by assessing factors such as premature saturation, overall signal intensity, and potential matrix effects in blank wells. Ultimately, the finalized method employed 1  $\mu$ g/mL anti-exatecan mAb and mouse anti-human IgG Fab Conjugate HRP diluted at 1:4000. The method has undergone comprehensive validation, with results falling within acceptable standards. This provides a basis for the bioanalysis of ADC drugs with exatecan as the payload. Exatecan, as a cytotoxic small molecule, typically exhibits reactivity by binding to immune effectors such as antibodies or cytokines. However, it inherently lacks immunogenicity, meaning it does not naturally stimulate an immune response. Immunogenicity is only induced when exatecan is chemically conjugated to an immune carrier to form a complete antigen. In the preparation of mouse anti-exatecan antibodies, BSA served as the protein carrier and was chemically conjugated with exatecan. During the mouse immunization phase, BSA conjugated with exatecan were selected as immunogens and combined with adjuvants in a specific ratio for mouse immunization. This structural integration ensures optimal epitope presentation, which effectively triggering an immune response and facilitating efficient antibody production. However, during the immunization process using BSA-exatecan as the immunogen to induce antibody production, antibodies targeting not only exatecan but also the linker and BSA were generated. To overcome this challenge, a competitive ELISA approach was employed during the hybridoma screening process. Specifically, in addition to allowing candidate antibodies to directly bind to BSA-exatecan, a certain concentration of free exatecan small molecule was introduced to compete for antibody binding. By comparing the binding signals under these two conditions, we successfully identified hybridoma cell lines capable of producing antibodies with specificity toward exatecan.

Exatecan is widely used as a cytotoxic component in antibody-drug conjugates for cancer research. The extensive use of exatecan necessitates the establishment of appropriate bioanalytical methods to effectively measure target analytes. The production of anti-exatecan monoclonal antibody can serve as a crucial reagent in these analytical methods, effectively binding to target analytes containing exatecan. The anti-exatecan mAb developed in this study has been employed in multiple experimental projects at Junshi Biosciences, yielding promising results and highlighting its potential for broader applications. In the parallelism experiment, the ADC quantification assay utilizing this antibody produced consistent results across various sample dilutions, demonstrating its reliability and reproducibility. These findings strongly support its application in preclinical PK and toxicokinetic (TK) evaluations.

Due to the unique structure and complexity of ADCs, bioanalysis encounters several challenges, such as potential alteration of the chemical structure of small molecule toxins during biotransformation and metabolism in the body. A limitation of this study is that exatecan, as a camptothecin derivative, has a lactone ring as its primary active

moiety, which is structurally unstable and prone to opening and closing under different pH conditions. The anti-payload antibody cannot react equally with both forms of the molecule, leading to inaccurate measurements of the conjugated drug [32,33]. Therefore, in ADC drug testing, the potential impact of the open and closed ring forms of the small molecule must be carefully considered. For practical application, this method needs further refinement in conjunction with actual ADC drugs and its implementation in pharmacokinetic studies. By comparing ADC quantification in animal serum samples with total antibody quantification, the feasibility of this method can be evaluated, and potential optimizations can be identified. The method of parallelism experiment involved acidifying the samples to allow binding under pH 3.0 conditions. This approach was designed to mitigate the potential impact of exatecan’s ring-opening and ring-closing conversion under different pH conditions, thereby ensuring more accurate quantification of the ADC. While this method has demonstrated applicability in preclinical research on exatecan-conjugates, its suitability for clinical studies remains uncertain. Specifically, the transition from preclinical to clinical settings introduces potential challenges, as the methods performance in human samples has not yet been validated. If transitioning to clinical settings, adjustments may be required. In clinical research, data obtained using bioanalytical methods are critical for evaluating the pharmacokinetics and pharmacodynamics of drugs in humans, which is essential for designing dosage, dosing frequency, and duration in clinical trials. Moreover, this study did not evaluate endogenous analytes in cynomolgus monkey serum samples. The future should witness the implementation of experimental tests similar to Feng Yin’s [34] investigation, which employed the PYX-201 total antibody method in pharmacokinetic and toxicology study. The analysis of structural changes in exatecan and their effects on ADC quantification in actual samples is critical. Variations in exatecan structure within biological systems, as well as the impact of sample pre-treatment, have not yet been replicated in this analytical method. Therefore, the practical application of this method requires further refinement in conjunction with actual ADC drugs. Since this method focuses on preclinical exatecan-conjugates research, its translation from preclinical to clinical settings warrants careful consideration. In clinical sample analysis, sensitivity, specificity, and lower limits of quantification are crucial. Clinical trials necessitate comprehensive pharmacokinetic and pharmacodynamic studies, alongside immunogenicity and safety assessments, thereby requiring the development of multiple bioanalytical methods.

Finally, this study successfully produced a high-quality 8B5-3H6 positive cell line using hybridoma technology and purified the monoclonal antibody (anti-exatecan mAb) from this cell line. The purity and affinity of this antibody were evaluated using SEC-HPLC and BLI, respectively, confirming its high purity and strong affinity. This antibody was subsequently employed to develop a bioanalytical method for antibody-exatecan conjugates. This monoclonal antibody can serve as a key reagent widely applicable in the detection of ADC drugs with exatecan as the payload, fulfilling the needs for subsequent toxicology and pharmacokinetic studies.

#### Author agreement statement

We the undersigned declare that this manuscript is original, has not been published before and is not currently being considered for publication elsewhere. We confirm that the manuscript has been read and approved by all named authors and that there are no other persons who satisfied the criteria for authorship but are not listed. We further confirm that the order of authors listed in the manuscript has been approved by all of us. We understand that the Corresponding Author is the sole contact for the Editorial process. He/she is responsible for communicating with the other authors about progress, submissions of revisions and final approval of proofs.

## CRediT authorship contribution statement

**Xu Junshuang & Wen Jing:** Writing – review & editing, Writing – original draft, Methodology, Validation. **Ji Xiaobo:** Formal analysis, Methodology. **Chen Jieru:** Methodology, Validation. **Yang Meiyu:** Investigation, Supervision. **Hong Min:** Writing – review & editing, Supervision, Project administration, Conceptualization. **Deng Dawei:** Resources, Supervision.

## Funding

This research did not receive any specific grant from funding agencies in the public, commercial, or not-for-profit sectors.

## Declaration of Competing Interest

The authors declare that they have no known competing financial interests or personal relationships that could have appeared to influence the work reported in this paper.

## Acknowledgements

The authors would like to thank Shanghai Junshi Biosciences Co., Ltd and China Pharmaceutical University resource support, we thank colleagues involved in the operation of this study.

## Appendix A. Supporting information

Supplementary data associated with this article can be found in the online version at [doi:10.1016/j.jpba.2025.116843](https://doi.org/10.1016/j.jpba.2025.116843).

## References

- [1] C.M. Mckertish, V. Kayser, Advances and limitations of antibody drug conjugates for cancer, *Biomedicines* 9 (2021) 872, <https://doi.org/10.3390/biomedicines9080872>.
- [2] C.H. Chau, P.S. Steeg, W.D. Figg, Antibody–drug conjugates for cancer, *Lancet* 394 (2019) 793–804, [https://doi.org/10.1016/s0140-6736\(19\)31774-x](https://doi.org/10.1016/s0140-6736(19)31774-x).
- [3] J.Z. Drago, S. Modi, S. Chandarlapaty, Unlocking the potential of antibody–drug conjugates for cancer therapy, *Nat. Rev. Clin. Oncol.* 18 (2021) 1–18, <https://doi.org/10.1038/s41571-021-00470-8>.
- [4] Z. Wang, H. Li, L. Gou, W. Li, Y. Wang, Antibody–drug conjugates: recent advances in payloads, *Acta Pharm. Sin. B* 13 (2023), <https://doi.org/10.1016/j.apsb.2023.06.015>.
- [5] J. Amani, N. Gorjizadeh, S. Younesi, M. Najafi, A.M. Ashrafi, S. Irian, N. Gorjizadeh, K. Azizian, Cyclin-dependent kinase inhibitors (CDKIs) and the DNA damage response: the link between signaling pathways and cancer, *DNA Repair* 102 (2021) 103103, <https://doi.org/10.1016/j.dnarep.2021.103103>.
- [6] S.J. Keam, Trastuzumab deruxtecan: first approval, *Drugs* 80 (2020) 501–508, <https://doi.org/10.1007/s40265-020-01281-4>.
- [7] Y.Y. Syed, Sacituzumab govitecan: first approval, *Drugs* 80 (2020) 1019–1025, <https://doi.org/10.1007/s40265-020-01337-5>.
- [8] S. Modi, C. Saura, T. Yamashita, Y.H. Park, S.-B. Kim, K. Tamura, F. Andre, H. Iwata, Y. Ito, J. Tsurutani, J. Sohn, N. Denduluri, C. Perrin, K. Aogi, E. Tokunaga, S.-A. Im, K.S. Lee, S.A. Hurvitz, J. Cortes, C. Lee, Trastuzumab deruxtecan in previously treated HER2-positive breast cancer, *N. Engl. J. Med.* 382 (2020) 610–621, <https://doi.org/10.1056/nejmoa1914510>.
- [9] K. Shitara, Y.-J. Bang, S. Iwasa, N. Sugimoto, M.-H. Ryu, D. Sakai, H.-C. Chung, H. Kawakami, H. Yabusaki, J. Lee, K. Saito, Y. Kawaguchi, T. Kamio, A. Kojima, M. Sugihara, K. Yamaguchi, Trastuzumab deruxtecan in previously treated HER2-positive gastric cancer, *N. Engl. J. Med.* 382 (2020) 2419–2430, <https://doi.org/10.1056/nejmoa2004413>.
- [10] C. for D.E. and Research, FDA grants accelerated approval to fam-trastuzumab deruxtecan-nxki for HER2-mutant non-small cell lung cancer, FDA, 2022. (<http://www.fda.gov/drugs/resources-information-approved-drugs/fda-grants-accelerated-approval-fam-trastuzumab-deruxtecan-nxki-her2-mutant-non-small-cell-lung>).
- [11] Center, FDA grants accelerated approval to fam-trastuzumab deruxtecan-nxki for, U.S. FDA, 2024. (<https://www.fda.gov/drugs/resources-information-approved-drugs/fda-grants-accelerated-approval-fam-trastuzumab-deruxtecan-nxki-unresectable-or-metastatic-her2>).
- [12] W. Dong, J. Shi, T. Yuan, B. Qi, J. Yu, J. Dai, L. He, Antibody–drug conjugates of 7-ethyl-10-hydroxycamptothecin: sacituzumab govitecan and labetuzumab govitecan, *Eur. J. Med. Chem.* 167 (2019) 583–593, <https://doi.org/10.1016/j.ejmech.2019.02.017>.
- [13] T. Nakada, T. Masuda, H. Naito, M. Yoshida, S. Ashida, K. Morita, H. Miyazaki, Y. Kasuya, Y. Ogitani, J. Yamaguchi, Y. Abe, T. Honda, Novel antibody drug conjugates containing exatecan derivative-based cytotoxic payloads, *Bioorg. Med. Chem. Lett.* 26 (2016) 1542–1545, <https://doi.org/10.1016/j.bmcl.2016.02.020>.
- [14] X. Jianyan, Z. Ying, C. Xiaofeng, Q. Bolei, L. Jindong, Z. Lianshan, H. Feng, T. Weikang, Ligand–drug conjugate of exatecan analogue, preparation method thereof and application thereof, [P], WO2020063676A1, 2020.
- [15] Z. Xiquan, C. Tianxi, F. Weiwei, Z. Bing, T. Xiaoqi, X. Tongjie, Antibody drug conjugate, [P], WO2022033578A1, 2022.
- [16] Z. Yi, W. Weili, Z. Guili, Y. Tianzi, Z. Shi, Y. Xiujian, Camptothecin derivative and ligand–drug conjugate thereof, [P], WO2022078260A1, 2022.
- [17] G.K. Abou-Alfa, L. Schwartz, S. Ricci, D. Amadori, A. Santoro, A. Figer, J. De Greve, J.-Y. Douillard, C. Lathia, B. Schwartz, I. Taylor, M. Moscovicci, L.B. Saltz, Phase II study of sorafenib in patients with advanced hepatocellular carcinoma, *J. Clin. Oncol.* 24 (2006) 4293–4300, <https://doi.org/10.1200/jco.2005.01.3441>.
- [18] W. Li, K.H. Veale, Q. Qiu, K.W. Sinkevicius, E.K. Maloney, J.A. Costoplus, J. Lau, H. L. Evans, Y. Setiady, O. Ab, S.M. Abbott, J. Lee, S. Wisitpitthaya, A. Skaletskaya, L. Wang, T.A. Keating, Ravi, W.C. Widdison, Synthesis and evaluation of camptothecin antibody–drug conjugates, *ACS Med. Chem. Lett.* 10 (2019) 1386–1392, <https://doi.org/10.1021/acsmchemlett.9b00301>.
- [19] S. Hejmady, R. Pradhan, S. Kumari, M. Pradhan, S.K. Dubey, R. Taliyan, Pharmacokinetics and toxicity considerations for antibody–drug conjugates: an overview, *Bioanalysis* 15 (2023) 1193–1202, <https://doi.org/10.4155/bio-2023-0104>.
- [20] Q. Qin, L. Gong, Current analytical strategies for antibody–drug conjugates in biomatrices, *Molecules* 27 (2022) 6299, <https://doi.org/10.3390/molecules27196299>.
- [21] G. Köhler, C. Milstein, Continuous cultures of fused cells secreting antibody of predefined specificity, *Nature* 256 (1975) 495–497, <https://doi.org/10.1038/256495a0>.
- [22] C. Zhang, Hybridoma technology for the generation of monoclonal antibodies, *Methods Mol. Biol.* 901 (2012) 117–135, [https://doi.org/10.1007/978-1-61779-931-0\\_7](https://doi.org/10.1007/978-1-61779-931-0_7).
- [23] E.A. Greenfield, Generating monoclonal antibodies, *pdb. top103036*, Cold Spring Harb. Protoc. 2022 (2022), <https://doi.org/10.1101/pdb.top103036>.
- [24] E.A. Greenfield, Electro cell fusion for hybridoma production, *pdb. prot103184*, Cold Spring Harb. Protoc. 2019 (2019), <https://doi.org/10.1101/pdb.prot103184>.
- [25] J. Ao, L. Wenli, S. Chuchu, Z. Shizhong, L. Yuying, Z. Pengqi, G. Cuicui, L. Xueting, Z. Mei, F. Hui, Linker for antibody–drug conjugate and use thereof, [P], WO2024056101A1, 2024.
- [26] Q. Sun, J. Luo, L. Zhang, Z. Zhang, T. Le, Development of monoclonal antibody-based ultrasensitive enzyme-linked immunosorbent assay and fluorescence-linked immunosorbent assay for 1-aminohydantoin detection in aquatic animals, *J. Pharm. Biomed. Anal.* 147 (2018) 417–424, <https://doi.org/10.1016/j.jpba.2017.06.068>.
- [27] C. Hollander, S.C. Walrond, C. Connelly, L. Megson, E. Bove, T. McDonagh, A custom ÄKTA avant configuration enabling automated parallel protein purification over a range of process scales, *Protein Expr. Purif.* 182 (2021) 105842, <https://doi.org/10.1016/j.pep.2021.105842>.
- [28] International Council for Harmonisation of Technical Requirements for Pharmaceuticals for Human Use. ICH Harmonised Guideline, Bioanalytical Method Validation M10, 2022.
- [29] FDA (US). Bioanalytical Method Validation Guidance for Industry, 2018.
- [30] B. Gorovits, S.C. Alley, S. Bilic, B. Booth, S. Kaur, P. Oldfield, S. Purushothama, C. Rao, S. Shord, P. Siguenza, Bioanalysis of antibody–drug conjugates: American association of pharmaceutical scientists antibody–drug conjugate working group position paper, *Bioanalysis* 5 (2013) 997–1006, <https://doi.org/10.4155/bio.13.38>.
- [31] Clinical pharmacology considerations for antibody–drug conjugates guidance for industry, March 28, 2024. (<https://www.fda.gov/regulatory-information/search-fda-guidance-documents/clinical-pharmacology-considerations-antibody-drug-conjugates-guidance-industry>).
- [32] U.Y. Lau, L.T. Benoit, N.S. Stevens, K.K. Emmerton, M. Zaval, J.H. Cochran, P. D. Senter, Lactone stabilization is not a necessary feature for antibody conjugates of camptothecins, *Mol. Pharm.* 15 (2018) 4063–4072, <https://doi.org/10.1021/acs.molpharmaceut.8b00477>.
- [33] Y. Zhang, X. Yun, L. Ouyang, X. Zhang, L. Gong, Q. Qin, Development of an ELISA with acidification treatment for an antibody conjugate incorporating exatecans, *Anal. Biochem.* 690 (2024), <https://doi.org/10.1016/j.ab.2024.115530>.
- [34] F. Yin, C. DeCiantis, J. Pinkas, B. Das, F. Wang, N. Zheng, D. Hahn, A. Amrite, J. Feng, D. Adhikari, C. Kane, J. Sikora, J. Pittman, R. Wates, E. Shaheen, S. Harriman, Quantitation of total antibody (tAb) from antibody drug conjugate (ADC) PYX-201 in rat and monkey plasma using an enzyme-linked immunosorbent assay (ELISA) and its application in preclinical studies, *J. Pharm. Biomed. Anal.* 233 (2023), <https://doi.org/10.1016/j.jpba.2023.115452>.